Electron optical-phonon coupling in GaAs/Al_xGa_{1-x}As quantum wells due to interface, slab, and half-space modes

G. Q. Hai, F. M. Peeters, and J. T. Devreese*

Departement Natuurkunde, Universiteit Antwerpen (UIA), Universiteitsplein 1, B-2610 Antwerpen, Belgium

(Received 14 April 1993)

The electron optical-phonon coupling is studied in GaAs/Al_xGa_{1-x}As quantum wells as due to the interface modes, the confined slab modes in the well, and the half-space modes in the barriers. The polaron binding energy and effective mass are calculated and the relative importance of the different phonon modes is investigated as a function of the width of the quantum well. The full-energy spectrum, i.e., the discrete energy levels in the well and the continuum energy spectrum above the barrier, are included as intermediate states. The polaron binding energy and effective mass go continuously from the three-dimensional (3D) Al_xGa_{1-x}As to the 3D GaAs results when the well width varies from zero to infinity.

I. INTRODUCTION

In a quasi-two-dimensional (Q2D) semiconductor system, such as heterojunctions, quantum wells, and superlattices, the phonon modes become much more complex than those in a three-dimensional (3D) system due to the presence of the interfaces. In most of the works about the problem of electron optical-phonon interaction in Q2D semiconductor systems, one assumed that the phonon modes were not influenced by the presence of the interfaces and the usual Fröhlich Hamiltonian based on the bulk phonons was employed. Recently, the optical-phonon modes in a Q2D semiconductor structure system have been studied and the electron-phonon interaction Hamiltonian was derived.[1–5] In the absence of external fields, several theoretical results have been obtained on polarons in Q2D systems where interface and slab phonon modes are included.[6–10] In Ref. 9, the present authors calculated the polaron energy and effective mass in a single quantum well. We found that, to obtain the correct results for narrow or wide quantum well structures, it is important to include the full energy spectrum as intermediate states in a second-order perturbation calculation of the polaron energy and effective mass. For an infinite-barrier quantum well model, it is possible to include all the intermediate states in the calculation. For a finite-barrier well model, however, the calculation becomes much more complicated and the so called leading term approximation was made in previous works. Within this approximation, the first important intermediate state is only taken into account and, as a consequence, it is impossible to obtain the correct results in the limit of well width.

In the presence of a magnetic field, we have studied the effect of interface and confined slab modes on the polaron Landau levels and the magneto-optical absorption spectrum in a GaAs/AlAs quantum well.[11] Our theoretical result demonstrated that in narrow GaAs/AlAs quantum wells a substantial coupling of the electrons with the interface phonon modes shows up near the LO- and TO-phonon modes of GaAs and AlAs at high magnetic fields.

In this paper, we will study the electron-phonon coupling in quantum wells due to the interface and the confined slab modes in the well, as well as the half-space modes in the barriers. The polaron binding energy and effective mass will be calculated and the relative importance of the different phonon modes will be investigated as a function of the width of the quantum well. This is the first calculation in which the full energy spectrum, i.e., the discrete energy levels in the well and the continuum energy spectrum above the barrier, are included as intermediate states and all the possible phonon modes which couple to the electrons are incorporated. Numerical results will be presented for a GaAs/Al_xGa_{1-x}As quantum well.

In Sec. II, we will give the Hamiltonian of the system and the bare electron states will be discussed in detail. Then, in Sec. III, the polaron binding energy and effective mass due to the different phonon modes will be calculated by including the full energy spectrum as intermediate states. Our results are summarized in Sec. IV, which also contains our conclusions.

II. THE HAMILTONIAN AND THE BARE ELECTRON STATES

The system under consideration is described by the Hamiltonian

$$H = \frac{\mathbf{p}^2}{2m_b} + V(z) + \sum_j \sum_{\mathbf{q}_\parallel} \hbar\omega_j(\mathbf{q}_\parallel)[a_j^\dagger(\mathbf{q}_\parallel)a_j(\mathbf{q}_\parallel) + \tfrac{1}{2}] + H_{ep}, \qquad (1)$$

where $\mathbf{p}$ $(\mathbf{r})$ is the momentum (position) operator of the electron, $a_j^\dagger(\mathbf{q}_\parallel)$ $[a_j(\mathbf{q}_\parallel)]$ the creation (annihilation) operator of an optical phonon with wave vector $\mathbf{q}_\parallel$ and energy $\hbar\omega_j(\mathbf{q}_\parallel)$ in the jth mode, and m_b the electron band mass which is given by

$$m_b = \begin{cases} m_{b1}, & |z| < W/2 \\ m_{b2}, & |z| > W/2, \end{cases} \tag{2}$$

where $m_{b1} = 0.067m_0$ and $m_{b2} = (0.067 + 0.083x)m_0$ are the electron band mass of GaAs and $Al_xGa_{1-x}As$, respectively, m_0 is the electron mass in vacuum, and W is the width of the quantum well. $V(z)$ is the confinement potential in the z direction,

$$V(z) = \begin{cases} 0, & |z| < W/2 \\ V_0, & |z| > W/2, \end{cases} \tag{3}$$

where $V_0 = 0.6 \times (1.155x + 0.37x^2)$ eV for the Γ point in a $GaAs/Al_xGa_{1-x}As$ quantum well. We denote GaAs as material 1 and $Al_xGa_{1-x}As$ as material 2. The material parameters[12] are given in Table I of Ref. 9. Notice that in $Al_xGa_{1-x}As$ there exist two pairs of LO- and TO-phonon modes (for $x \neq 0$ and $x \neq 1$); one is GaAs-like and the other is AlAs-like. In the present calculation we will make the effective LO- and TO-phonon mode approximation[12] which we expect to be valid in the nonresonant polaron region.

In a semiconductor heterostructure the phonon modes are modified because of the presence of the interfaces. For a single $GaAs/Al_xGa_{1-x}As$ quantum well structure, there are four types of optical-phonon modes which couple to the electrons: (1) the symmetric-interface-optical-phonon modes with frequency $\omega_{S\pm}(q_\parallel)$ ($j = S\pm$), (2) the antisymmetric-interface-optical-phonon modes with frequency $\omega_{A\pm}(q_\parallel)$ ($j = A\pm$), (3) the confined slab LO-phonon modes in the well with frequency ω_{L1} ($j = l$, l=1,2,3,...), and (4) the half-space LO-phonon modes in the barrier layers with frequency ω_{L2} ($j = q_z$).

The confined slab LO-phonon modes are dispersionless with frequency ω_{L1}, but their momentum in the z direction is quantized with $q_z = l\pi/W$, $l = 1, 2, 3, \ldots, l_{\max}$, where $l_{\max} = \text{int}(W/a_0)$ and $a_0 = 5.65$ Å is the lattice constant of GaAs.

The electron-phonon interaction Hamiltonian can be written in the form[1,2,9]

$$H_{ep} = \sum_j \sum_{\mathbf{q}_\parallel} e^{i\mathbf{q}_\parallel \cdot \mathbf{r}_\parallel} \Gamma_j(\mathbf{q}_\parallel, z)[a_j(\mathbf{q}_\parallel) + a_j^\dagger(-\mathbf{q}_\parallel)] , \tag{4}$$

where $\Gamma_j(\mathbf{q}_\parallel, z)$ is the coupling function which describes the coupling strength of a single electron at the position z with the jth optical-phonon mode with the dispersion relation $\omega_j(q_\parallel)$. The expression of the coupling function was given by Eqs. (13)–(17) in Ref. 9.

The state of a bare electron in such a system is determined by the Hamiltonian $H_e = \mathbf{p}^2/2m_b + V(z)$. The eigenenergy of the bare electron is

$$E^0 = E_\parallel + E_z, \tag{5}$$

and the corresponding wave function can be written as

$$\Psi(x, y, z) = \phi(x, y)\psi(z), \tag{6}$$

where $\phi(x, y)$ is the wave function in the xy plane and $\psi(z)$ the one in the z direction as determined by $V(z)$. In the following we will discuss the electron energy and wave function which are important to calculate the polaron energy and effective mass due to the electron-phonon interaction in detail.

A. Discrete energy levels in the well

An electron in a quantum well has discrete levels $E_z = E_n^z < V_0$, which are determined by the transcendental equation

$$\tan\left(\frac{W}{2}\frac{\sqrt{2m_{b1}E_n^z}}{\hbar}\right) = \left(\frac{m_{b1}(V_0 - E_n^z)}{m_{b2}E_n^z}\right)^{1/2} \tag{7}$$

for $n = 1, 3, 5, \ldots$. These levels correspond to the symmetric wave function

$$\psi_n(z) = \begin{cases} B_n \cos(k_n z), & |z| \le W/2 \\ B_n \cos(k_n W/2)e^{-k_n'(|z|-W/2)}, & |z| > W/2 , \end{cases} \tag{8}$$

where $k_n = \sqrt{2m_{b1}E_n^z}/\hbar$, $k_n' = \sqrt{2m_{b2}(V_0 - E_n^z)}/\hbar$, and the normalization constant

$$B_n = \left(\frac{2k_n}{k_nW + \sin(k_nW) + 2k_n\cos^2(k_nW/2)/k_n'}\right)^{1/2} . \tag{9}$$

The equation

$$\cot\left(\frac{W}{2}\frac{\sqrt{2m_{b1}E_n^z}}{\hbar}\right) = -\left(\frac{m_{b1}(V_0 - E_n^z)}{m_{b2}E_n^z}\right)^{1/2} \tag{10}$$

determines the energy levels $n = 2, 4, 6, \ldots$, and the corresponding wave functions are antisymmetric,

$$\psi_n(z) = \begin{cases} A_n \sin(k_n z), & |z| \le W/2 \\ \text{sgn}(z)A_n \sin(k_n W/2)e^{-k_n'(|z|-W/2)}, & |z| > W/2 , \end{cases} \tag{11}$$

with the normalization constant

$$A_n = \left(\frac{2k_n}{k_nW - \sin(k_nW) + 2k_n\sin^2(k_nW/2)/k_n'}\right)^{1/2} . \tag{12}$$

B. Continuum energy spectrum above the barrier V_0

We consider the case that the total sample length L_z is much larger than the well width W; in fact, we will assume that $L_z \to \infty$. In such a situation the eigenenergy has a continuum spectrum above the barrier V_0. We find that there exist two types of states, i.e., the symmetric one with wave function

$$\psi_S(z) = \frac{B'}{\sqrt{L_z}} \begin{cases} \cos(k_W z), & |z| \le W/2 \\ \cos(k_W W/2)\cos[k_B(|z|-W/2)] - \xi^{-1}\sin(k_W W/2)\sin[k_B(|z|-W/2)], & |z| > W/2\ , \end{cases} \tag{13}$$

and the antisymmetric one with wave function

$$\psi_A(z) = \frac{A'}{\sqrt{L_z}} \begin{cases} \sin(k_W z), & |z| \le W/2 \\ \mathrm{sgn}(z)\{\sin(k_W W/2)\cos[k_B(|z|-W/2)] + \xi^{-1}\cos(k_W W/2)\sin[k_B(|z|-W/2)]\}, & |z| > W/2\ , \end{cases} \tag{14}$$

where $k_W = \sqrt{2m_{b1}E_z}/\hbar$, $k_B = \sqrt{2m_{b2}(E_z - V_0)}/\hbar$, $\xi = m_{b1}k_B/m_{b2}k_W$,

$$B' = \left\{\frac{1}{2}\left[\cos^2\left(\frac{k_W W}{2}\right) + \xi^{-2}\sin^2\left(\frac{k_W W}{2}\right)\right]\right\}^{-1/2}, \tag{15}$$

and

$$A' = \left\{\frac{1}{2}\left[\sin^2\left(\frac{k_W W}{2}\right) + \xi^{-2}\cos^2\left(\frac{k_W W}{2}\right)\right]\right\}^{-1/2}. \tag{16}$$

The energy $E_\parallel$ in the xy plane in Eq. (5) can be written as

$$E_\parallel = \frac{\hbar^2 k_\parallel^2}{2m_\parallel}, \tag{17}$$

where $\mathbf{k}_\parallel$ is the electron wave vector and $m_\parallel$ the effective mass in the xy plane which is given by

$$m_\parallel = \frac{m_{b1}m_{b2}}{P_w m_{b2} + P_b m_{b1}}, \tag{18}$$

where P_w (P_b) is the probability of finding the electron inside (outside) the quantum well. The corresponding wave function $\phi(x,y)$ has the form

$$\phi_{\mathbf{k}_\parallel}(x,y) = \frac{1}{\sqrt{A}} e^{i\mathbf{k}_\parallel\cdot\mathbf{r}_\parallel}. \tag{19}$$

III. THE POLARON ENERGY AND EFFECTIVE MASS

In this section, we will calculate the polaron correction to the ground state energy and its effective mass within second-order perturbation theory. The energy of a polaron in the ground state is given by

$$E = E_\parallel + E_1^z - \Delta E, \tag{20}$$

where ΔE is the energy shift due to electron-phonon interaction. The effective mass is given by

$$m = m_\parallel + \Delta m, \tag{21}$$

with Δm the correction due to the electron-phonon interaction.

Based on second-order perturbation theory the polaron contribution to the binding energy and the effective mass is given by

$$\Delta E = \frac{A}{2\pi}\sum_n\sum_j\int_0^\infty dq_\parallel \times \frac{q_\parallel |M_{1,n}^j(\mathbf{q}_\parallel)|^2}{\hbar\omega_j(q_\parallel) + E_z - E_1^z + \hbar^2 q_\parallel^2/2m_\parallel} \tag{22a}$$

and

$$\Delta m = \frac{A}{2\pi}\sum_n\sum_j\int_0^\infty dq_\parallel \frac{\hbar^2 q_\parallel^3 |M_{1,n}^j(\mathbf{q}_\parallel)|^2}{[\hbar\omega_j(q_\parallel) + E_z - E_1^z + \hbar^2 q_\parallel^2/2m_\parallel]^3}, \tag{22b}$$

respectively, with the electron-phonon interaction matrix element

$$\begin{aligned} M_{1,n}^j(\mathbf{q}_\parallel) &= \langle \mathbf{k}_\parallel - \mathbf{q}_\parallel, n; \mathbf{q}|H_{ep}|\mathbf{k}_\parallel, 1; 0\rangle \\ &= \langle n|\Gamma_j(\mathbf{q}_\parallel, z)|1\rangle, \end{aligned} \tag{23}$$

which has to be calculated for the different phonon modes and the full set of intermediate states. Notice that the sum over n in Eq. (22) is an abbreviation for all the possible electron energy states in the system, which are the discrete levels in the well and the continuum energy spectrum above the barrier. For the continuum energy spectrum the sum over n transforms into an integration.

A. Confined slab phonon modes

1. The contribution from the discrete energy levels

The contribution of the electron–slab-phonon interaction to the polaron energy and effective mass from the discrete levels E_n^z in the well is given by

$$\Delta E_{\rm slab}^{\rm disc} = 2\alpha_1\hbar\omega_{L1}(m_\parallel/m_{b1})k_{\rm LO}W \times \sum_{n=1}^{n_{\rm max}}\sum_{l=1}^{l_{\rm max}} |G_{1,n}^l|^2 F_l(E_n^z) \tag{24}$$

and

$$\Delta m_{\rm slab}^{\rm disc} = 4\alpha_1 (m_{\parallel}^3/m_{b1}^2) k_{\rm LO}^3 W^3 \sum_{n=1}^{n_{\rm max}} \sum_{l=1}^{l_{\rm max}} |G_{1,n}^l|^2 P_l(E_n^z), \tag{25}$$

respectively, where $k_{\rm LO} = (2m_{b1}\omega_{L1}/\hbar)^{1/2}$, $n_{\rm max} = {\rm int}(W\sqrt{2m_{b1}V_0}/\hbar\pi) + 1$ is the number of the discrete levels in the quantum well,

$$G_{1,n}^l = \begin{cases} B_1 B_n \left[\dfrac{l\pi W \cos[(k_1 - k_n)W/2]}{(l\pi)^2 - [(k_1 - k_n)W]^2} + \dfrac{l\pi W \cos[(k_1 + k_n)W/2]}{(l\pi)^2 - [(k_1 + k_n)W]^2} \right], & n, l = \text{odd} \\ B_1 A_n \left[\dfrac{l\pi W \sin[(k_1 - k_n)W/2]}{(l\pi)^2 - [(k_1 - k_n)W]^2} - \dfrac{l\pi W \sin[(k_1 + k_n)W/2]}{(l\pi)^2 - [(k_1 + k_n)W]^2} \right], & n, l = \text{even}, \end{cases} \tag{26}$$

otherwise $G_{1,n}^l = 0$;

$$F_l(E) = \frac{\ln[\eta(E)/l^2\pi^2]}{[\eta(E) - l^2\pi^2]} \tag{27}$$

and

$$P_l(E) = \frac{1}{[l^2\pi^2 - \eta(E)]^2} \left(\frac{\ln[\eta(E)/l^2\pi^2]}{1 - \eta(E)/l^2\pi^2} + \frac{l^2\pi^2}{2\eta(E)} + \frac{1}{2} \right), \tag{28}$$

where

$$\eta(E) = 2m_{\parallel} W^2 (\hbar\omega_{L1} + E - E_1^z)/\hbar^2. \tag{29}$$

2. The contribution from the continuum energy spectrum

The contribution of the electron–slab-phonon interaction to the polaron energy and effective mass from the continuum states $E_z > V_0$ is given by

$$\Delta E_{\rm slab}^{\rm cont} = \alpha_1 (\hbar\omega_{L1})^{1/2} \left(\frac{m_{\parallel}}{m_{b1}} \right) \frac{k_{\rm LO}^2 W}{\pi} \int_{V_0}^{\infty} dE_z \frac{1}{\sqrt{E_z}} \sum_{l=1}^{l_{\rm max}} |G^l(k_W)|^2 F_l(E_z) \tag{30}$$

and

$$\Delta m_{\rm slab}^{\rm cont} = 2\alpha_1 (\hbar\omega_{L1})^{-1/2} \left(\frac{m_{\parallel}^3}{m_{b1}^2} \right) \frac{k_{\rm LO}^4 W^3}{\pi} \int_{V_0}^{\infty} dE_z \frac{1}{\sqrt{E_z}} \sum_{l=1}^{l_{\rm max}} |G^l(k_W)|^2 P_l(E_z), \tag{31}$$

respectively, where

$$G^l(k_W) = \begin{cases} B_1 B' \left[\dfrac{l\pi W \cos[(k_1 - k_W)W/2]}{(l\pi)^2 - [(k_1 - k_W)W]^2} + \dfrac{l\pi W \cos[(k_1 + k_W)W/2]}{(l\pi)^2 - [(k_1 + k_W)W]^2} \right], & l = \text{odd} \\ B_1 A' \left[\dfrac{l\pi W \sin[(k_1 - k_W)W/2]}{(l\pi)^2 - [(k_1 - k_W)W]^2} - \dfrac{l\pi W \sin[(k_1 + k_W)W/2]}{(l\pi)^2 - [(k_1 + k_W)W]^2} \right], & l = \text{even}, \end{cases} \tag{32}$$

and $F_l(E)$ and $P_l(E)$ are given by Eqs. (27) and (28). Then, the polaron binding energy and effective mass correction due to the electron–slab-phonon coupling are given by

$$\Delta E_{\rm slab} = \Delta E_{\rm slab}^{\rm disc} + \Delta E_{\rm slab}^{\rm cont}, \tag{33}$$

and

$$\Delta m_{\rm slab} = \Delta m_{\rm slab}^{\rm disc} + \Delta m_{\rm slab}^{\rm cont}, \tag{34}$$

which are depicted in Figs. 1 and 2, respectively, as a function of the well width for a $GaAs/Al_{0.3}Ga_{0.7}As$ quantum well. Both $\Delta E_{\rm slab}^{\rm disc}$ and $\Delta E_{\rm slab}^{\rm cont}$ are zero at $W = 0$ as one expects. With increasing well width, $\Delta E_{\rm slab}^{\rm disc}$ increases monotonously while $\Delta E_{\rm slab}^{\rm cont}$ is zero up to $W = a_0$ and then starts to increase rapidly in the range $W < 50$ Å before the second discrete level appears in the quantum well, the position of which is indicated by the arrow labeled by $n = 2$ in Fig. 1(a). After the third level appears, $\Delta E_{\rm slab}^{\rm cont}$ starts to oscillate very weakly. We find that $\Delta E_{\rm slab}^{\rm disc}$ has a discontinuous derivative each time a new level enters the quantum well, and at the same time

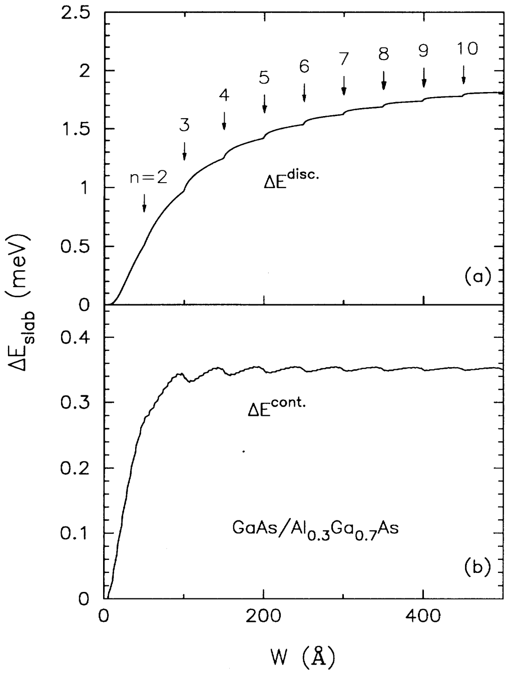

FIG. 1. The confined slab phonon mode contribution to the polaron binding energy from (a) the discrete levels in the well, and (b) the continuum states above the barrier for a $GaAs/Al_{0.3}Ga_{0.7}As$ quantum well structure. The arrows indicate the position at which a new discrete level appears. The number n gives the number of discrete levels in the quantum well.

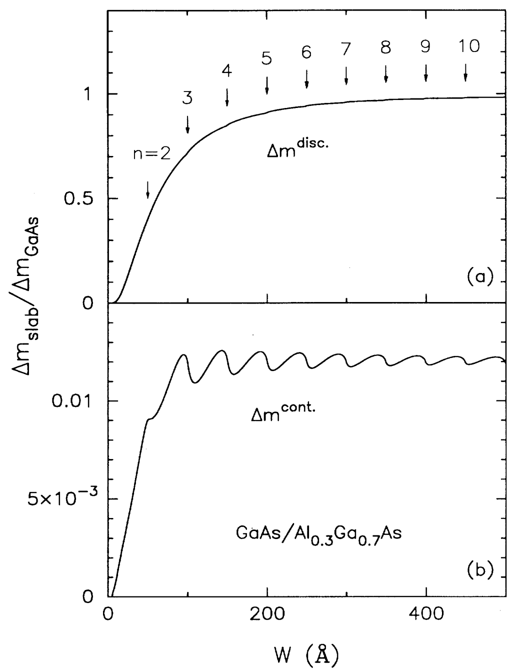

FIG. 2. The same as Fig. 1 but for the polaron effective mass.

$\Delta E_{\rm slab}^{\rm cont}$ decreases. The small structure in Fig. 1(b) occurs for $W = la_0, l = 1, 2, 3, \ldots$, which is a consequence of each time a new slab mode enters the quantum well with increasing the well width. For very wide wells $\Delta E_{\rm slab}$ approaches the 3D result of GaAs as it should be. The corresponding results for the polaron mass are shown in Figs. 2(a) and 2(b). We denote the polaron mass correction with respect to the 3D GaAs value $\Delta m_{\rm GaAs} = \alpha_1 m_{b1}/6$. Notice that the contribution of the continuum part of the spectrum to the polaron correction for the energy and the mass is always smaller than the corresponding contribution from the discrete part.

B. The symmetric-interface-phonon modes

1. *The contribution from the discrete energy levels*

The contribution of the electron–symmetric-interface-phonon interaction to the polaron energy and effective mass from the discrete levels E_n^z in the well is given by

$$\Delta E_S^{\rm disc} = \frac{\alpha_1 \hbar\omega_{L1}}{k_{\rm LO}(1/\epsilon_{\infty 1} - 1/\epsilon_{01})} \sum_{+,-} \sum_{n=1}^{n_{\max}} \int_0^\infty dq_\parallel |G_{1,n}^S(q_\parallel)|^2 F_{S,\pm}(q_\parallel, E_n^z) \tag{35}$$

and

$$\Delta m_S^{\rm disc} = \frac{\alpha_1 \hbar\omega_{L1}}{k_{\rm LO}(1/\epsilon_{\infty 1} - 1/\epsilon_{01})} \sum_{+,-} \sum_{n=1}^{n_{\max}} \int_0^\infty dq_\parallel |G_{1,n}^S(q_\parallel)|^2 P_{S,\pm}(q_\parallel, E_n^z), \tag{36}$$

where

$$G_{1,n}^S(q_\parallel) = B_1 B_n \left\{ q_\parallel \left[\frac{\cos[(k_1+k_n)W/2]}{(k_1+k_n)^2 + q_\parallel^2} + \frac{\cos[(k_1-k_n)W/2]}{(k_1-k_n)^2 + q_\parallel^2} \right] \tanh\left(\frac{q_\parallel W}{2}\right) + \frac{(k_1+k_n)\sin[(k_1+k_n)W/2]}{(k_1+k_n)^2 + q_\parallel^2} + \frac{(k_1-k_n)\sin[(k_1-k_n)W/2]}{(k_1-k_n)^2 + q_\parallel^2} + \frac{2\cos(k_1 W/2)\cos(k_n W/2)}{k_1' + k_n' + q_\parallel} \right\}, \tag{37}$$

for n=odd, and $G^S_{1,n}(q_\parallel) = 0$ for n=even,

$$F_{S,\pm}(q_\parallel, E) = \frac{(1+e^{-q_\parallel W})B_{S,\pm}(q_\parallel)}{\omega_{S,\pm}(q_\parallel)[\omega_{S,\pm}(q_\parallel) + (E - E^z_1)/\hbar + \hbar q^2_\parallel/2m_\parallel]}, \tag{38}$$

$$P_{S,\pm}(q_\parallel, E) = \frac{q^2_\parallel(1+e^{-q_\parallel W})B_{S,\pm}(q_\parallel)}{\omega_{S,\pm}(q_\parallel)[\omega_{S,\pm}(q_\parallel) + (E - E^z_1)/\hbar + \hbar q^2_\parallel/2m_\parallel]^3}, \tag{39}$$

and

$$B_{S,\pm}(q_\parallel) = \frac{[\omega^2_{T1} - \omega^2_{S,\pm}(q_\parallel)]^2[\omega^2_{T2} - \omega^2_{S,\pm}(q_\parallel)]^2}{\epsilon^S_1(\omega^2_{L1} - \omega^2_{T1})[\omega^2_{T2} - \omega^2_{S,\pm}(q_\parallel)]^2 + \epsilon^S_2(\omega^2_{L2} - \omega^2_{T2})[\omega^2_{T1} - \omega^2_{S,\pm}(q_\parallel)]^2}, \tag{40}$$

where $\epsilon^S_1 = \epsilon_{\infty 1}(1 - e^{-q_\parallel W})$ and $\epsilon^S_2 = \epsilon_{\infty 2}(1 + e^{-q_\parallel W})$.

2. The contribution from the continuum energy spectrum

The contribution of the electron–symmetric-interface-phonon interaction to the polaron energy and effective mass from the continuum states $E_z > V_0$ is given by

$$\Delta E^{\rm cont}_S = \frac{\alpha_1(\hbar\omega_{L1})^{1/2}}{2\pi(1/\epsilon_{\infty 1} - 1/\epsilon_{01})} \sum_{+,-} \int_{V_0}^{\infty} dE_z \frac{1}{\sqrt{E_z}} \int_0^\infty dq_\parallel |G^S(q_\parallel)|^2 F_{S,\pm}(q_\parallel, E_z) \tag{41}$$

and

$$\Delta m^{\rm cont}_S = \frac{\alpha_1(\hbar\omega_{L1})^{1/2}}{2\pi(1/\epsilon_{\infty 1} - 1/\epsilon_{01})} \sum_{+,-} \int_{V_0}^{\infty} dE_z \frac{1}{\sqrt{E_z}} \int_0^\infty dq_\parallel |G^S(q_\parallel)|^2 P_{S,\pm}(q_\parallel, E_z), \tag{42}$$

where

$$\begin{aligned} G^S(q_\parallel) = B_1 B' \Bigg\{ & q_\parallel \left[\frac{\cos[(k_1 + k_W)W/2]}{(k_1 + k_W)^2 + q^2_\parallel} + \frac{\cos[(k_1 - k_W)W/2]}{(k_1 - k_W)^2 + q^2_\parallel} \right] \tanh\left(\frac{q_\parallel W}{2}\right) \\ & + \frac{(k_1 + k_W)\sin[(k_1 + k_W)W/2]}{(k_1 + k_W)^2 + q^2_\parallel} + \frac{(k_1 - k_W)\sin[(k_1 - k_W)W/2]}{(k_1 - k_W)^2 + q^2_\parallel} \\ & + \frac{2\cos(k_1 W/2)}{k^2_B + (k'_1 + q_\parallel)^2} \left[(k'_1 + q_\parallel)\cos\left(\frac{k_W W}{2}\right) - \xi^{-1} k_B \sin\left(\frac{k_W W}{2}\right) \right] \Bigg\}, \end{aligned} \tag{43}$$

and $F_{S,\pm}(q_\parallel, E)$ and $P_{S,\pm}(q_\parallel, E)$ are given by Eqs. (38) and (39), respectively. Then we obtain the contribution to the polaron energy due to the symmetric interface modes

$$\Delta E_S = \Delta E^{\rm disc}_S + \Delta E^{\rm cont}_S, \tag{44}$$

and the contribution to the polaron mass

$$\Delta m_S = \Delta m^{\rm disc}_S + \Delta m^{\rm cont}_S. \tag{45}$$

C. The antisymmetric-interface-phonon modes

The contribution from the antisymmetric-interface-phonon modes to the polaron energy and mass is much smaller than the previous one. For the discrete levels in the well, we have

$$\langle 1|\Gamma_{A,\pm}(\mathbf{q}_\parallel, z)|1\rangle = 0 \tag{46}$$

and the antisymmetric interface modes have a very small contribution to the polaron energy and mass only when the second level $n = 2$ appears (this is for $W \simeq 50$ Å in GaAs/$Al_{0.3}Ga_{0.7}As$ and for $W \simeq 25$ Å in GaAs/AlAs quantum well). We will neglect this part and take $\Delta E^{\rm disc}_A = 0$ and $\Delta m^{\rm disc}_A = 0$.

For the continuum energy spectrum $E_z > V_0$, we obtain

$$\Delta E^{\rm cont}_A = \frac{\alpha_1(\hbar\omega_{L1})^{1/2}}{2\pi(1/\epsilon_{\infty 1} - 1/\epsilon_{01})} \times \sum_{+,-} \int_{V_0}^{\infty} dE_z \frac{1}{\sqrt{E_z}} \times \int_0^\infty dq_\parallel |G^A(q_\parallel)|^2 F_{A,\pm}(q_\parallel, E_z), \tag{47}$$

and

$$\Delta m_A^{\rm cont} = \frac{\alpha_1(\hbar\omega_{L1})^{1/2}}{2\pi(1/\epsilon_{\infty 1} - 1/\epsilon_{01})} \sum_{+,-} \int_{V_0}^{\infty} dE_z \frac{1}{\sqrt{E_z}} \int_0^{\infty} dq_{\|} |G^A(q_{\|})|^2 P_{A,\pm}(q_{\|}, E_z), \tag{48}$$

where

$$G^A(q_{\|}) = B_1 A' \Bigg\{ q_{\|} \left[\frac{\sin[(k_1 + k_W)W/2]}{(k_1 + k_W)^2 + q_{\|}^2} - \frac{\sin[(k_1 - k_W)W/2]}{(k_1 - k_W)^2 + q_{\|}^2} \right] \coth\left(\frac{q_{\|}W}{2}\right) + \frac{(k_1 - k_W)\cos[(k_1 - k_W)W/2]}{(k_1 - k_W)^2 + q_{\|}^2} - \frac{(k_1 + k_W)\cos[(k_1 - k_W)W/2]}{(k_1 + k_W)^2 + q_{\|}^2} + \frac{2\cos(k_1 W/2)}{k_B^2 + (k_1' + q_{\|})^2} \left[(k_1' + q_{\|}) \sin\left(\frac{k_W W}{2}\right) + \xi^{-1} k_B \cos\left(\frac{k_W W}{2}\right) \right] \Bigg\}, \tag{49}$$

$$F_{A,\pm}(q_{\|}, E) = \frac{(1 - e^{-q_{\|}W}) B_{A,\pm}(q_{\|})}{\omega_{A,\pm}(q_{\|})[\omega_{A,\pm}(q_{\|}) + (E - E_1^z)/\hbar + \hbar q_{\|}^2/2m_{\|}]}, \tag{50}$$

$$P_{A,\pm}(q_{\|}, E) = \frac{q_{\|}^2(1 - e^{-q_{\|}W}) B_{A,\pm}(q_{\|})}{\omega_{A,\pm}(q_{\|})[\omega_{A,\pm}(q_{\|}) + (E - E_1^z)/\hbar + \hbar q_{\|}^2/2m_{\|}]^2}, \tag{51}$$

and

$$B_{A,\pm}(q_{\|}) = \frac{[\omega_{T1}^2 - \omega_{A,\pm}^2(q_{\|})]^2 [\omega_{T2}^2 - \omega_{A,\pm}^2(q_{\|})]^2}{\epsilon_1^A(\omega_{L1}^2 - \omega_{T1}^2)[\omega_{T2}^2 - \omega_{A,\pm}^2(q_{\|})]^2 + \epsilon_2^A(\omega_{L2}^2 - \omega_{T2}^2)[\omega_{T1}^2 - \omega_{A,\pm}^2(q_{\|})]^2}, \tag{52}$$

where $\epsilon_1^A = \epsilon_{\infty 1}(1 + e^{-q_{\|}W})$ and $\epsilon_2^A = \epsilon_{\infty 2}(1 - e^{-q_{\|}W})$.

For GaAs/$Al_{0.3}Ga_{0.7}As$ quantum well structures, the energies $\Delta E_S^{\rm disc}$ and $\Delta E_S^{\rm cont}$ and $\Delta E_A^{\rm cont}$ are given as a function of the well width in Figs. 3(a) and 3(b), respectively. It is shown that, with increasing well width, the interface mode contribution starts from zero at $W = 0$ and increases to a maximum at $W \simeq 20$ Å ($\Delta E_S^{\rm disc}$), 5 Å ($\Delta E_S^{\rm cont}$), and 27 Å ($\Delta E_A^{\rm cont}$), then decreases to zero. The corresponding results for the polaron mass are shown in Fig. 4. The behavior of the polaron mass correction due to the interface modes is similar to the one of the binding energy. The maximum of $\Delta m_S^{\rm disc}$ ap-

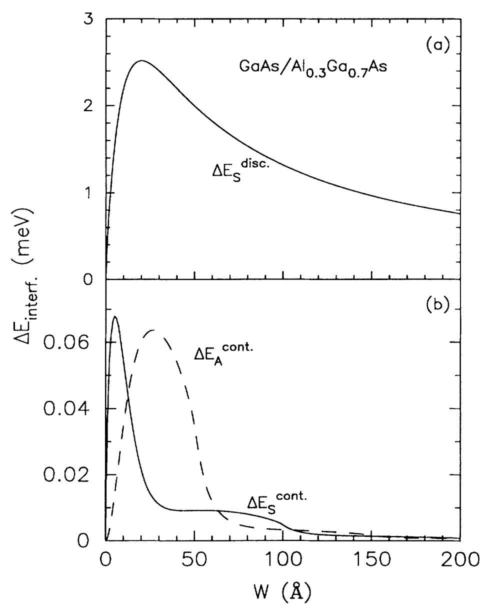

FIG. 3. The interface phonon mode contribution to the polaron energy from (a) the discrete levels in the well, and (b) the continuum states above the barrier in a GaAs/$Al_{0.3}Ga_{0.7}As$ quantum well structure. The solid and dashed curves in (b) indicate the contribution from the symmetric ($\Delta E_S^{\rm cont}$) and the antisymmetric ($\Delta E_A^{\rm cont}$) phonon modes, respectively.

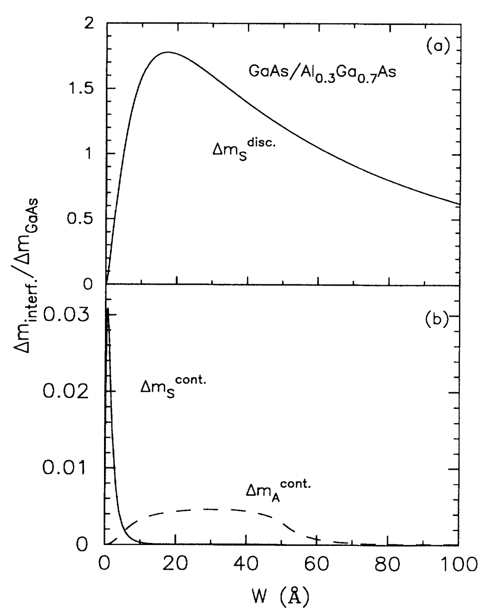

FIG. 4. The same as Fig. 3 but for the polaron effective mass.

pears at $W \simeq 18$ Å, and those of $\Delta m_S^{\rm cont}$ and $\Delta m_A^{\rm cont}$ at $W \simeq 1$ Å and $W \simeq 25$ Å, respectively. Notice that the contribution from the electron states in the continuum is very small. The interface modes are important for not too wide and not too narrow quantum wells.

D. The half-space phonon modes

The half-space phonon modes are only important for very narrow quantum wells because only then is there an appreciable overlap between the electron wave function and the phonons in the barrier. In this case only one or a few discrete energy levels exist in the quantum well. Furthermore we have

$$\langle 1|\Gamma_{L2}(\mathbf{q}_\|, q_z; z)|1\rangle = 0, \quad (53)$$

and consequently only the coupling via the continuum energy spectrum $E_z > V_0$ is important. We obtain

$$\Delta E_{\rm half} = \frac{\alpha_2}{\pi^2}(\hbar\omega_{L2})^{3/2}\int_{V_0}^\infty \frac{dE_z}{\sqrt{E_z - V_0}}\int_0^\infty dq_z \frac{|G_{\rm half}|^2 \ln[(\hbar^2 q_z^2/2m_{b2})/(\hbar\omega_{L2} + E_z - E_1^z)]}{\hbar^2 q_z^2/2m_{b2} - (\hbar\omega_{L2} + E_z - E_1^z)}, \quad (54)$$

and

$$\Delta m_{\rm half} = \frac{\alpha_2}{\pi^2}(\hbar\omega_{L2})^{3/2}\int_{V_0}^\infty \frac{dE_z}{\sqrt{E_z - V_0}}\int_0^\infty dq_z \int_0^\infty dx \frac{\hbar^2 x |G_{\rm half}|^2}{(q_z^2 + x)(\hbar\omega_{L2} + E_z - E_1^z + \hbar^2 x/2m_\|)^3}, \quad (55)$$

where

$$G_{\rm half} = B_1 A' \cos\left(\frac{k_1 W}{2}\right) \frac{q_z(q_z^2 + k_1'^2 - k_B^2)\sin(k_W W/2) + 2\xi^{-1}k_1 k_B q_z \cos(k_W W/2)}{[(k_B + q_z)^2 + k_1'^2][(k_B - q_z)^2 + k_1'^2]}. \quad (56)$$

We have calculated the contribution of the electron–half-space-phonon interaction to the polaron binding energy (the dotted curves in Fig. 5) and effective mass (the dotted curves in Fig. 6) through the continuum energy states in GaAs/$Al_{0.3}Ga_{0.7}As$ and GaAs/AlAs quantum wells. With increasing well width, the contributions due to half-space modes to the polaron energy and mass decreases rapidly from the 3D values of $Al_xGa_{1-x}As$ at $W = 0$ to zero for $W \to \infty$.

IV. SUMMARY AND CONCLUSION

So far, we have calculated the separate contributions from the electron coupling to the different phonon modes to the polaron energy and effective mass including the full energy spectrum as intermediate states. The polaron binding energy and effective mass in a quantum well system is thus given by

$$\Delta E = \Delta E_{\rm slab} + \Delta E_S + \Delta E_A + \Delta E_{\rm half}, \quad (57)$$

and

$$\Delta m = \Delta m_{\rm slab} + \Delta m_S + \Delta m_A + \Delta m_{\rm half}. \quad (58)$$

The results of the polaron binding energy for (a) a GaAs/$Al_{0.3}Ga_{0.7}As$ and (b) a GaAs/AlAs quantum well structure are shown in Figs. 5(a) and 5(b), respectively. And the results of the polaron effective mass are presented in Figs. 6(a) and 6(b). The contribution from the confined slab phonon, the interface phonon, and the half-space phonon modes are given by the thin-solid, the dot-dashed and the dotted curves, respectively. Clearly, the half-space modes are important for very narrow quantum wells and, in such cases, their contribution to the polaron is only via the continuum energy states above the bar-

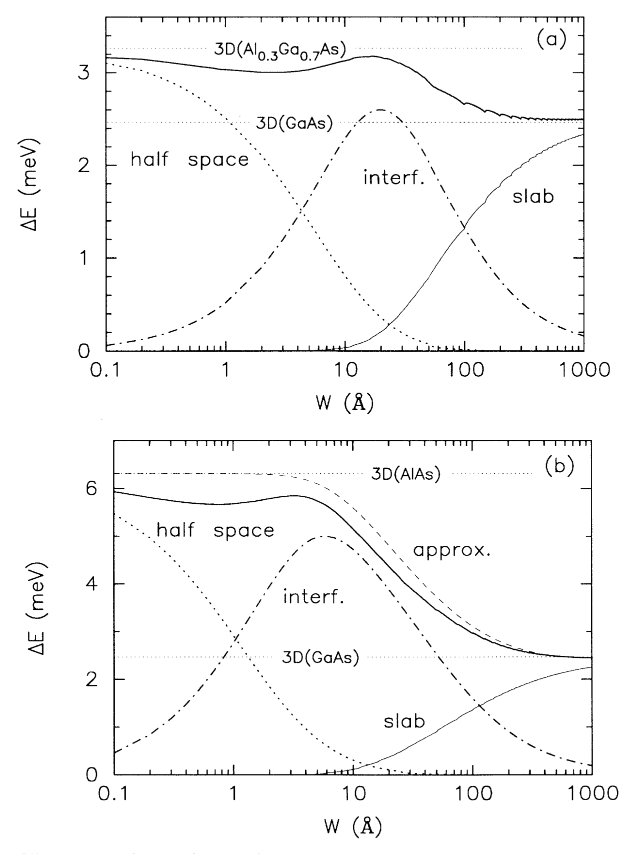

FIG. 5. The polaron binding energy as a function of the well width for (a) GaAs/$Al_{0.3}Ga_{0.7}As$ and (b) GaAs/AlAs quantum-well structures. The thin-solid, dot-dashed, and dotted curves indicate the contribution from the slab, interface, and half-space modes, respectively. The thick-solid curves give the total polaron binding energy. The thin-dashed curve in (b) is the approximate result as given in Ref. 9.

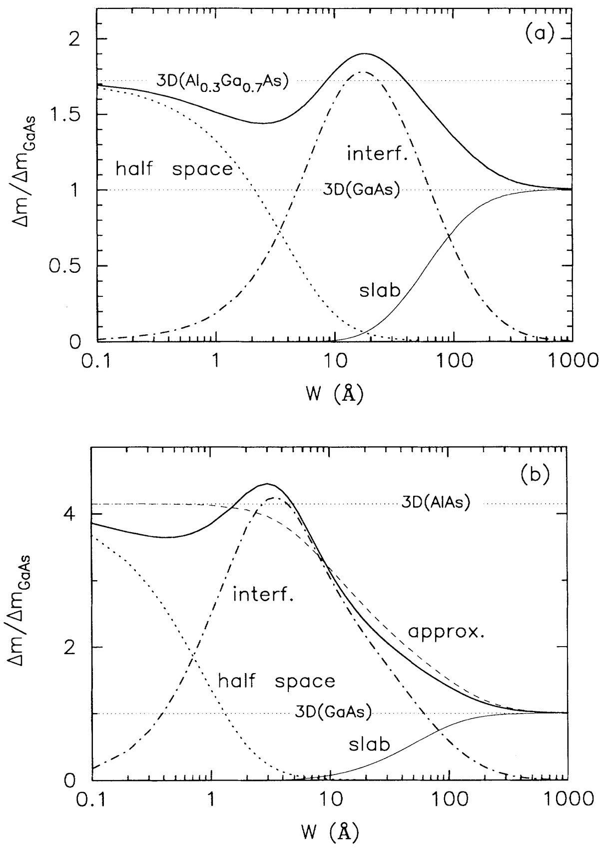

FIG. 6. The same as Fig. 5 but for the polaron effective mass.

rier. When $W \to 0$, $\Delta E \to \Delta E_{\mathrm{half}}$ which approaches the 3D result of the barrier material $Al_xGa_{1-x}As$. With increasing well width the ΔE_{half} decreases rapidly and the interface mode contribution becomes important. For $W \geq 100$ Å, the slab mode contribution is larger than that of the interface modes. Our calculation demonstrates that the polaron binding energy and effective mass go continuously from the 3D $Al_xGa_{1-x}As$ to the 3D GaAs results when the well width varies from zero to infinity. The thin-dashed curves in Figs. 5(b) and 6(b) are the approximate results as given by Eqs. (42)–(45) in Ref. 9 which were based on the calculation of the polaron effects in an infinite-barrier quantum well[13] where the results were weighted by the probability to find the electron inside the finite-barrier quantum well.

As far as we know, the present paper is the first work which includes the full energy spectrum and all the possible phonon modes in the study of the polaron effects in a Q2D system. Within the infinite-well model, Comas, Trallero-Giner, and Riera[6] calculated the polaron binding energy and effective mass including only the confined slab modes, and Degani and Hipólito[7,8] incorporated the interface and confined slab modes to study the polarons in a heterojunction and a quantum well. The shortcoming of the infinite-well model is that the electrons have no coupling to the half-space modes and, furthermore, when the well width goes to zero, an ideal 2D system is reached instead of the realistic 3D system. More recently, Lin, Chen, and George[10] studied the polaron ground state in a GaAs/AlAs quantum well. Within the leading term approximation, the confined slab and the interface modes, as well as the half-space modes, were incorporated in their calculation. They claimed erroneously that the $W \to 0$ and $W \to \infty$ limit results were obtained correctly. In Ref. 10 the polaron binding energy and the effective mass were given for a GaAs/AlAs quantum well for $W < 100$ Å which were much smaller than the 3D values of GaAs. From the present results and from Ref. 9 we know that this cannot be the case and the full electron energy spectrum has to be included.

ACKNOWLEDGMENTS

One of us (F.M.P.) is supported by the Belgian National Science Foundation. This work is sponsored by Fonds voor Kollektief Fundamenteel Onderzoek, Belgium, Project No. 2.0093.91, and by "Diensten voor de Programmatie van het Wetenschapsbeleid" (Belgium) under Contract No. IT/SC/24.

---

* Also at RUCA, B-2020 Antwerpen, Belgium, and Technical University of Eindhoven, The Netherlands.

[1] L. Wendler, Phys. Status Solidi B **129**, 513 (1985).

[2] L. Wendler and R. Pechstedt, Phys. Status Solidi B **141**, 129 (1987).

[3] N. Mori and T. Ando, Phys. Rev. B **40**, 6175 (1989).

[4] K. Haung and B. F. Zhu, Phys. Rev. B **38**, 13 377 (1988).

[5] J. J. Licari and R. Evrard, Phys. Rev. B **15**, 2254 (1977).

[6] F. Comas, C. Trallero-Giner, and R. Riera, Phys. Rev. B **39**, 5907 (1989).

[7] M. H. Degani and O. Hipólito, Phys. Rev. B **35**, 7717 (1987).

[8] M. H. Degani and O. Hipólito, Superlatt. Microstruct. **5**, 141 (1989).

[9] G. Q. Hai, F. M. Peeters, and J. T. Devreese, Phys. Rev. B **42**, 11 063 (1991).

[10] D. L. Lin, R. Chen, and Thomas F. George, J. Phys. Condens. Matter **3**, 4645 (1991).

[11] G. Q. Hai, F. M. Peeters, and J. T. Devreese, Physica B **184**, 289 (1993).

[12] S. Adachi, J. Appl. Phys. **58**, R1 (1985).

[13] Equations (42) and (43) in Ref. 9 should be replaced by $\Delta E_{\mathrm{barrier}} = (1 - P)\alpha_2\hbar\omega_{L2}$ and $\Delta m^*_{\mathrm{barrier}} = (1 - P)\alpha_2 m_{b2}/6$, respectively. The solid curves in Figs. 5(a) and 5(b) in Ref. 9 should be replaced by the thin-dashed curves in Figs. 5(b) and 6(b) of the present paper.